The dipolar Frenkel excitonic insulator phase of an impurity in a liquid solvent: results

1993 J. Phys.: Condens. Matter 5 3121

(http://iopscience.iop.org/0953-8984/5/19/011)

J. Phys.: Condens. Matter 5 (1993) 3121–3138. Printed in the UK

The dipolar Frenkel excitonic insulator phase of an impurity in a liquid solvent: results

M D Winn and D E Logan†
Physical Chemistry Laboratory, Oxford University, South Parks Road, Oxford OX1 3QZ, UK

Received 16 February 1993

Abstract. In a previous paper we have developed a mean field theory for the dipolar Frenkel excitonic insulator (EI) phase of an impurity at infinite dilution in a liquid solvent or disordered matrix, a situation of experimental relevance. Based on this, we here present numerical results for the location of the EI transition, and the impurity dipole moment in the dipolar EI phase, using linear classical liquid state theories. For a non-polar polarizable solvent, we consider impurity and solvent atoms of (i) identical hard-sphere diameter, and (ii) differing hard-sphere diameter. We also generalize the previously studied model to allow for dipolar polarizable solvent molecules, and present example results. We consider in particular the case of alkali metal atoms dissolved in methylamine, and conclude that a dipolar EI phase is possible for Li and Cs.

1. Introduction

In two previous papers [1,2] (hereafter referred to as I and II), we have developed the theory of a dipolar Frenkel excitonic insulator (EI). In I, we introduced the model system, and described two alternative analyses of it. The first, termed 'pairing theory', is the more rigorous, but suffers from two disadvantages. First, although it is able to locate the point at which a system is unstable with respect to a Frenkel EI phase, it cannot describe the EI phase itself. Second, the full pairing theory (including 'double-excitation' terms) is readily soluble only for lattice-based systems. The second analysis does not have these disadvantages, but the Hartree decoupling of electronic operators upon which it is based requires some justification. This was largely achieved in I, where excellent agreement with pairing theory was found for lattice-based examples.

In II, we therefore extended the Hartree analysis to spatially disordered systems. For a given atomic configuration, diagonalization of the Hartree Hamiltonian gave a self-consistency relation for the atomic dipole moments, a non-zero solution to which implies a dipolar EI phase. An explicit expression was found for the dipole moment of an impurity at infinite dilution in a solvent, again for a given atomic configuration. The ensemble of atomic configurations was then taken into account via a mean field approximation. The results presented in II were given in terms of the average reaction field factor of the system, a microscopic prescription for which was described. One purpose of the present paper is to give explicit results based on calculations of the average reaction field factor, using linear classical liquid state theories. This is the subject of section 2.

The possibility of a Frenkel EI phase occurring in impurity systems has been suggested by results from a number of experiments [3–5]. In addition, a quantum molecular dynamics

† e-mail address: dlogan@uk.ac.ox.vax

0953-8984/93/193121+18$07.50

simulation [6] of Na in molten NaBr yielded a dipolar atomic state for the excess Na, in contrast to the F-centre-like states found for the heavier alkali metals. More recently, there has been experimental support for this finding [5]. We also mention the path integral Monte Carlo simulations of Li in liquid ammonia [7, 8]. The first calculation [7] yielded a dipolar Li atom [9], while a more recent calculation [8] with different model potentials predicted, in contrast, that Li ionizes in liquid ammonia. This latter result is, in fact, more in keeping with experimental results on the alkali metals in liquid ammonia (see, for example, [10]). In the dilute regime, those results that are attributable to the electron are independent of the cation involved, and one consequently infers ionization of the alkali metal atom with at most loose pairing between the solvated cation and the solvated electron.

Liquid ammonia is, however, only one of a large range of solvents, most notably amines and ethers, in which the alkali metals form a dilute solution [10], and these other solvents are likely to be better candidates for the observation of a Frenkel EI phase. The dielectric constant of amines and ethers is generally lower than that of ammonia, and the cation–electron interaction is consequently stronger. Hence, the alkali metal impurities do not necessarily ionize, and evidence has emerged for a variety of distinguishable species that may arise from a single metal atom, ranging from a loose ion pair to a solvated atom [10]. Further species arise when more than one alkali atom is involved, but in the present study we are solely concerned with a single impurity.

The alkali metal species that have been distinguished in these systems are, however, invariably assumed to be spherically symmetric. What we suggest in this paper, via some example calculations, is that non-spherically symmetric species (dipolar atoms) are a further possibility.

Most of the experimentally studied impurity systems described above involve a solvent species possessing a permanent dipole moment, and such systems cannot be described by the atom-based model studied in I and II. The generalization, within the class of linear liquid state theories, to dipolar polarizable solvents is, however, relatively straightforward. The necessary formalism is set out in section 3.1, and some sample results are given in section 3.2. We find that the probability of a dipolar impurity is greatly enhanced by a dipolar solvent. Finally, a short summary is given in section 4.

2. Numerical examples for non-polar solvent

The mean field solution pertaining to the dipolar EI phase of an atomic impurity in a non-polar polarizable solvent was derived in II. The impurity dipole moment, μ_i, is given explicitly in terms of the transition dipole moment of the impurity atom, M_i, the static polarizability of an isolated impurity atom, α_{i0}, and the average reaction field factor associated with the solvent, G, as follows. When $\alpha_{i0}G < 1$, the only solution is

$$\mu_i = 0 \tag{2.1}$$

i.e. the non-dipolar state of the impurity. When $\alpha_{i0}G > 1$, however, there is a further solution

$$\frac{|\mu_i|^2}{M_i^2} = 1 - \frac{1}{\alpha_{i0}^2 G^2} \tag{2.2}$$

representing a dipolar impurity state that is energetically stable with respect to the non-dipolar state. The central quantity in a calculation of μ_i is clearly G, and a microscopic

prescription for this quantity was given in II in terms of the solvent number density, ρ, and the renormalized static polarizability of a solvent atom in the condensed phase, α. In calculating G, the average is taken over a spherically symmetric reference potential, which we here assume to be of hard-sphere form.

The calculation of G is necessarily approximate, and in the present paper we consider solely the class of linear approximations of classical liquid state theory. Before presenting the results of specific linear theories, we mention again two properties, discussed in II, that a well behaved theory should reproduce. First, for linear theories, and when the impurity and solvent atoms have an identical hard-core diameter σ, the Onsager saturation property [11] implies the inequality

$$G \leqslant 8/\sigma^3. \tag{2.3}$$

Using (2.2), this inequality implies an upper bound to $|\mu_i|$. Second, G is given to lowest order in $\rho\alpha$ by

$$\begin{aligned} G &= \rho\alpha \int \mathrm{d}\boldsymbol{R}\, g_2(R)\, \tfrac{1}{3}\mathrm{Tr}\big(\mathbf{T}(\boldsymbol{R})\mathbf{T}(-\boldsymbol{R})\big) + \mathrm{O}[(\rho\alpha)^2] \\ &= 8\pi\rho\alpha \int_0^\infty \mathrm{d}R\, R^{-4} g_2(R) + \mathrm{O}[(\rho\alpha)^2] \end{aligned} \tag{2.4}$$

where $g_2(R)$ is the pair distribution function appropriate to the hard-sphere potential, and

$$\mathbf{T}(\boldsymbol{R}) = \frac{3\boldsymbol{R}\boldsymbol{R}}{|\boldsymbol{R}|^5} - \frac{\mathbf{I}}{|\boldsymbol{R}|^3} \tag{2.5}$$

is the dipole–dipole interaction tensor, with $\mathbf{I}$ the identity matrix.

2.1. Equisized hard spheres

In this subsection we assume the hard-sphere diameters associated with solute–solvent and solvent–solvent interactions to be equal, and denoted by σ (unequal diameters are investigated in section 2.2). The advantage of assuming equal diameters is that the reference distribution functions are independent of whether a site is a solute or solvent atom. While this assumption may not appear realistic, we show in section 2.2 that the change in the numerical results upon adopting differing diameters can largely be accounted for simply by an appropriate choice of the reduced impurity polarizability in the calculation of this subsection.

We use σ to define the following set of reduced variables

$$\tilde{\alpha}_{i0} = \alpha_{i0}\sigma^{-3} \qquad \tilde{\alpha}_0 = \alpha_0\sigma^{-3} \qquad \tilde{\alpha} = \alpha\sigma^{-3} \qquad \rho^* = \rho\sigma^3 \qquad \tilde{G} = G\sigma^3 \tag{2.6}$$

where we have introduced α_0, the static polarizability of an isolated solvent atom. In II, we showed that (for linear theories) G is precisely the quantity that relates the renormalized solvent polarizability, α, to the bare solvent polarizability, α_0. In terms of the above reduced variables, this relation is

$$\tilde{\alpha} = \tilde{\alpha}_0(1 - \tilde{G}\tilde{\alpha}_0)^{-1}. \tag{2.7}$$

The most convenient route for the calculation of G is thus via available theories for α. Different linear theories correspond to different closures to (2.7), and we now consider three such.

Possibly the most accurate linear theory is the SSCA of Wertheim [12], which corresponds to the reference version of Patey's LHNC [13]. This approximate theory is analytically soluble in one limit, namely when the reference pair distribution function, $g_2(R)$, is taken to be of step-function form. The relevant equations are then formally identical to those of the MSA for the case of non-polarizable dipolar molecules, and the closure to (2.7) is [12]

$$4\pi\rho^*\tilde{\alpha} = q(\tilde{G}/8) - q(-\tilde{G}/16) \tag{2.8}$$

where

$$q(x) = \frac{(1+2x)^2}{(1-x)^4}. \tag{2.9}$$

The right-hand side of (2.8) increases monotonically from 0 to ∞ as $\tilde{G}$ varies between 0 and 8. It follows from this that $\tilde{G}$, as determined from (2.7) and (2.8), is always less than 8, and the Onsager saturation property (2.3) is correctly reproduced. Thus, from (2.2) the value of $|\mu_i|$ predicted by the MSA has a limiting value of $M_i[1-(1/64\tilde{\alpha}_{i0}^2)]^{1/2}$. To lowest order in $\rho\alpha$, the MSA equations predict

$$\tilde{G} = \frac{8\pi}{3}\rho^*\tilde{\alpha} + O[(\rho\alpha)^2] \tag{2.10}$$

which is precisely (2.4) for the assumed case of a step-function $g_2(R)$.

The step-function form for $g_2(R)$ assumed by the MSA is not realistic, and we do not expect the MSA to give quantitatively reliable answers. An alternative closure to (2.7), which incorporates the effects of a realistic hard sphere $g_2(R)$, was used by Pratt [14], and is based on the free-energy Padé approximant of Rushbrooke and co-workers [15]. In the present notation, the closure relation is

$$\tilde{G} = 8\pi\rho^*\tilde{\alpha}I_2(\rho^*)\left(1+\frac{\rho^*\tilde{\alpha}I_3(\rho^*)}{2\pi I_2(\rho^*)}\right)^{-1} - 2(\rho^*\tilde{\alpha})^2 I_3(\rho^*)\left(1+\frac{\rho^*\tilde{\alpha}I_3(\rho^*)}{2\pi I_2(\rho^*)}\right)^{-2} \tag{2.11}$$

where

$$\begin{aligned} I_2(\rho^*) &= \frac{\sigma^3}{8\pi}\int \mathrm{d}\boldsymbol{R}\, g_2(R)\tfrac{1}{3}\mathrm{Tr}\left[\mathbf{T}(\boldsymbol{R})\mathbf{T}(-\boldsymbol{R})\right] \\ &= \sigma^3\int_0^\infty \mathrm{d}R\, R^{-4} g_2(R) \end{aligned} \tag{2.12}$$

and $I_3(\rho^*)$ is an analogous three-body integral. With $g_2(R)$ appropriate to a hard-sphere fluid, the following Padé approximants [14] give accurate values for these integrals over all realistic liquid densities:

$$I_2(\rho^*) = \frac{1}{3}\left(\frac{1-0.3618\rho^*-0.3205\rho^{*2}+0.1078\rho^{*3}}{(1-0.5236\rho^*)^2}\right) \tag{2.13}$$

$$I_3(\rho^*) = \frac{2.741\,56}{2.707\,97}\left(\frac{2.707\,97+1.689\,18\rho^*-0.3157\rho^{*2}}{1-0.590\,56\rho^*+0.200\,59\rho^{*2}}\right). \tag{2.14}$$

Note that these are the expressions appropriate to (2.11), and differ by constant factors from those given originally [16, 17]. The assumption of a step-function form for $g_2(R)$ is equivalent to setting $\rho^* = 0$ in (2.13) and (2.14).

The term $\tilde{G}$, as given by (2.11), is an unbounded function, and consequently $|\mu_i|$ has a limiting value of M_i, corresponding to the largest possible dipole moment obtainable within the assumed basis. Although the Onsager saturation property (2.3) is not recovered, it is in fact satisfied for all physical densities. As $\rho\alpha \to 0$, $\tilde{G}$ is given by

$$\tilde{G} = 8\pi\rho^*\tilde{\alpha}I_2(\rho^*) + O[(\rho\alpha)^2]. \tag{2.15}$$

With the identification (2.12), we see that the Padé approximant of Pratt reproduces fully the limit (2.4).

A second and simpler Padé approximant to $\tilde{G}$ was suggested by Chandler and co-workers [18]. These authors gave as the closure to (2.7)

$$\tilde{G} = 8\pi\rho^*\tilde{\alpha}I_2(\rho^*)\left(1 + \frac{\rho^*\tilde{\alpha}I_3(\rho^*)}{\pi I_2(\rho^*)}\right)^{-1} \tag{2.16}$$

where $I_2(\rho^*)$ and $I_3(\rho^*)$ are again given by (2.13) and (2.14). The behaviour of this approximant in the low-$\rho^*\tilde{\alpha}$ and high-$\tilde{\alpha}$ limits is identical to that of the Pratt approximant.

For the sake of comparison, we also give the form of $\tilde{G}$ when the solvent is treated as a continuum. From continuum dielectric theory [19], the reaction field factor is given by

$$G = \frac{2}{d^3}\frac{\epsilon - 1}{2\epsilon + 1} \tag{2.17}$$

where ϵ is the static dielectric constant of the solvent, and d is the radius of a cavity within which the impurity resides. To apply this expression, we must choose an appropriate value for d, and relate ϵ to ρ and α_0. We use Onsager's prescription for the cavity radius, $4\pi d^3/3 = 1/\rho$, and evaluate ϵ via the Clausius–Mossotti relation, obtaining

$$\tilde{G} = \frac{(32\pi^2/9)\rho^{*2}\tilde{\alpha}_0}{1 + (4\pi/3)\rho^*\tilde{\alpha}_0}. \tag{2.18}$$

As for the above Padé approximants, the $\tilde{G}$ predicted by continuum dielectric theory is unbounded, and $|\mu_i|$ again has a limiting value of M_i. Further, it is clear that (2.18) does not yield the correct low-density limit, being quadratic in ρ^* rather than linear. The spurious factor of ρ^* arises from the Onsager prescription for the cavity radius, d. An alternative choice for the cavity radius would be $d = \sigma$, whence we recover, in the low-density limit, (2.10) with α replaced by α_0, which is the correct limit for a structureless solvent. Unfortunately, (2.17) then yields unrealistically low values for $\tilde{G}$. We therefore do not consider further the $d = \sigma$ case.

We thus calculate the impurity dipole moment, $|\mu_i|/M_i$, from (2.1) ($\tilde{\alpha}_{i0}\tilde{G} < 1$) or (2.2) ($\tilde{\alpha}_{i0}\tilde{G} > 1$), and (2.7), with one of the above closure relations. The required input parameters are $\tilde{\alpha}_{i0}$, $\tilde{\alpha}_0$ and ρ^*. We postpone modelling of specific experimental systems until section 3, and here simply evaluate the above approximate theories for a physically sensible range of parameters.

In figures 1 and 2, we give sample results for $\tilde{\alpha}_{i0} = 0.889$. This value represents one of the most favourable cases for the formation of a dipolar impurity atom: that of a small polarizable impurity, e.g. Li ($\alpha_{i0} = 24\,\text{Å}^3$ [20]) with σ taken equal to 3 Å. In figure 1, for this choice of $\tilde{\alpha}_{i0}$ and for each approximate theory described above, we plot the values of the solvent parameters, ρ^* and $\tilde{\alpha}_0$, at which there is a transition from the normal insulating (non-dipolar) state to the Frenkel EI (dipolar) state. The region below (above) each line corresponds to values of ρ^* and $\tilde{\alpha}_0$ for which the impurity is in a non-dipolar (dipolar)

state. The range of ρ^* considered covers all physically realizable densities, and the range of $\tilde{\alpha}_0$ considered is typical of appropriate solvents.

It is clear that the formation of a dipole moment on the impurity site is favoured by high solvent density and high solvent polarizability. This is, of course, because a dense polarizable solvent produces a larger reaction field at a dipolar impurity site than a low-density weakly polarizable solvent. A dipolar impurity state is also favoured by a high impurity polarizability, and, as we have mentioned, the high value of $\tilde{\alpha}_{i0}$ that we have taken is one of the most favourable cases.

It is clear from figure 1 that, with $g_2(R)$ taken as a step function, the MSA and the two Padé approximants considered give comparable results. All predict that a dipolar impurity state exists only over a small range of reasonable solvent parameters. With a more realistic form for $g_2(R)$, however, both Padé approximants predict an increased likelihood of a dipolar phase, and there is a wide range of solvent parameters for which it occurs. Assuming the latter results to be the most reliable, it is clear that the MSA underestimates the likelihood of a dipolar state, and that this is due to the unrealistic form of $g_2(R)$ assumed. Finally, continuum dielectric theory clearly overestimates the likelihood of a dipolar state.

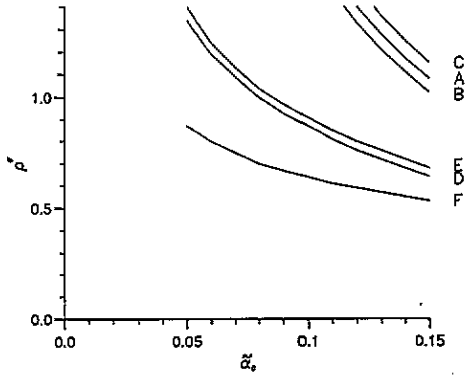

Figure 1. Values of the solvent parameters, ρ^* and $\tilde{\alpha}_0$, at which a transition from the normal insulating phase to the dipolar EI phase occurs, for $\tilde{\alpha}_{i0} = 0.889$. The results of the MSA (curve A), the Padé of Pratt [14] (B) and the Padé of Chandler and co-workers [18] (C) with a step function $g_2(R)$, the Padé of Pratt (D) and the Padé of Chandler and co-workers (E) with a realistic hard sphere $g_2(R)$, and of continuum dielectric theory (F) are shown.

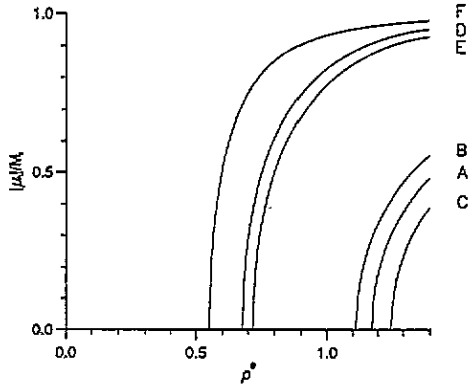

Figure 2. The reduced impurity dipole moment, $|\mu_i|/M_i$, as a function of ρ^*, for $\tilde{\alpha}_0 = 0.140$ and $\tilde{\alpha}_{i0} = 0.889$. The curves are labelled as in figure 1.

In figure 2, we illustrate the growth of the impurity dipole moment with solvent density, as predicted by each of the approximate theories considered, for $\tilde{\alpha}_{i0} = 0.889$ and $\tilde{\alpha}_0 = 0.140$. For densities slightly greater than the transition density, the dipole moment grows with the mean field exponent of 1/2. For higher densities the dipole moment saturates, as discussed earlier.

2.2. Different hard-sphere diameters

In this subsection, we relax the assumption of equal hard-sphere diameters. We denote the impurity–solvent hard-sphere diameter by σ_{is}, the solvent–solvent hard-sphere diameter by

σ_{ss}, and we further define an impurity–impurity diameter, σ_{ii}, via

$$\sigma_{is} = \tfrac{1}{2}(\sigma_{ss} + \sigma_{ii}). \tag{2.19}$$

We then define

$$\Sigma = \sigma_{ii}/\sigma_{ss} \tag{2.20}$$

which is the ratio of the 'size' of the impurity atom to the 'size' of the solvent atom.

The Padé approximants used in the previous subsection are based on the two- and three-body integrals, $I_2(\rho^*)$ and $I_3(\rho^*)$, and it is relatively straightforward to generalize these integrals to the case $\sigma_{is} \neq \sigma_{ss}$. However, the Padé approximants were designed so that these two integrals represent (approximately) higher-order terms in the expansion of G. To use modified versions of the two- and three-body integrals in the Padé approximants would thus be to overestimate the influence of a value of σ_{is} which differs from σ_{ss}. We do not therefore consider the Padé approximants in this subsection, and concentrate instead on the MSA solution for the case $\sigma_{is} \neq \sigma_{ss}$. We have seen in the previous subsection that, because of the simplistic form assumed for $g_2(R)$, the MSA underestimates the likelihood of a Frenkel EI phase. The results of the MSA are, however, not unreasonable, and allow one to gain an appreciation of the effects of unequal hard-sphere diameters.

The solution of the MSA for the case $\sigma_{is} \neq \sigma_{ss}$ is quite involved, and so we merely state the result here, assigning the derivation to the appendix. We choose the solvent–solvent diameter, σ_{ss}, to be the unit of length, and define reduced variables via (2.6) with σ replaced by σ_{ss}. The dipole moment on the impurity is given by equation (2.1) or (2.2), with G replaced by G^{is}, where G^{is} is defined to be the average reaction field factor determining the reaction field at the impurity site. We thus need to know $\alpha_{i0}G^{is} = \tilde{\alpha}_{i0}\tilde{G}^{is}$, and this is given by (see (A.27))

$$\tilde{\alpha}_{i0}\tilde{G}^{is} = \frac{4\pi\rho^*\tilde{\alpha}\tilde{\alpha}_{i0}\tilde{G}^{ss}}{q^{is}(\tilde{G}^{ss}/8) - q^{is}(-\tilde{G}^{ss}/16)}. \tag{2.21}$$

Here, the renormalized solvent polarizability, $\tilde{\alpha}$, is precisely the quantity calculated in the previous subsection, and $\tilde{G}^{ss}$ is the reaction field factor, which determines the reaction field at a solvent atom and which enters the calculation of $\tilde{\alpha}$; $\tilde{G}^{ss}$ equals $\tilde{G}^{is}$ only for the case $\sigma_{is} = \sigma_{ss}$. Finally, the function q^{is} is given by equations (A.28)–(A.31).

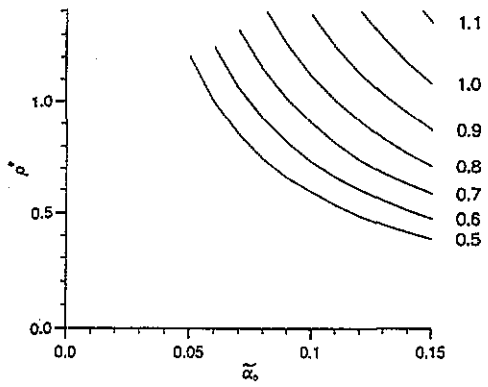

Figure 3. As figure 1, but for the MSA only. Curves are labelled by the value of $\Sigma = \sigma_{ii}/\sigma_{ss}$.

As an example, we again take the favourable value $\tilde{\alpha}_{i0} \equiv \alpha_{i0}\sigma_{ss}^{-3} = 0.889$, and consider the dependence of the impurity dipole moment on the size of the impurity, via its dependence on Σ. In figure 3, for this choice of $\tilde{\alpha}_{i0}$ and for various values of Σ, we plot the values of the solvent parameters, ρ^* and $\tilde{\alpha}_0$, at which there is a transition from the normal insulating state to the dipolar EI state, as calculated in the MSA. It is clear from figure 3 that the dipolar state is favoured by small values of Σ. This is as expected, since a small impurity atom (σ_{ii}, and hence Σ, small) permits a closer approach of the solvent atoms, consequently enhancing the reaction field.

Equation (2.21) can be written in the form

$$\tilde{\alpha}_{i0}\tilde{G}^{is} = \alpha_{i0}\sigma_{is}^{-3} \times \tfrac{1}{8}(1+\Sigma)^3\tilde{G}^{is} \tag{2.22}$$

The first factor on the right-hand side incorporates that part of the Σ dependence that reflects the closeness of approach of the solvent and impurity atoms; the remaining Σ dependence is included in the second factor. We can judge the relative contributions of these two factors to the overall Σ dependence by holding one of them fixed as Σ is varied, and doing so we find the Σ dependence of the second factor to be small. For example, holding the first factor $\alpha_{i0}\sigma_{is}^{-3}$ fixed at 0.889, and taking $\tilde{\alpha}_0 = 0.15$, the critical density at which a transition takes place is $\rho^* = 0.946$ for $\Sigma = 0.5$ and $\rho^* = 1.106$ for $\Sigma = 1.1$. The principal effect of changing the size of the impurity (i.e. Σ) is thus to change the closeness of approach of the solvent and impurity atoms, as embodied in a different value of $\alpha_{i0}\sigma_{is}^{-3}$, and the remaining Σ dependence can, to a good approximation, be neglected. In that case, we have $\tilde{\alpha}_{i0}\tilde{G}^{is} \simeq \alpha_{i0}\sigma_{is}^{-3} \times \tilde{G}^{ss}$, and the calculation is precisely as in section 2.1 but with $\tilde{\alpha}_{i0}$ replaced by an effective value $\alpha_{i0}\sigma_{is}^{-3}$.

3. Extension to polar solvents

3.1. Formalism

The results of section 2, based on the theory of II, pertain to a model in which both impurity and solvent sites are atomic in nature, with a four-level electronic basis. In arriving at the final solution, the electronic degrees of freedom are integrated out, leaving a classical problem given in terms of the polarizabilities of the impurity atom, α_{i0}, and the solvent atoms, α_0. Strictly speaking, these polarizabilities are those corresponding to the assumed four-level basis, but in practice we have treated the polarizabilities as input parameters obtained from experiment. In a similar way, although we have assumed the solvent to be atomic, it seems admissible to generalize the results obtained to dipolar polarizable solvent molecules. As discussed in section 1, this significantly increases the range of systems we may model.

We showed in II that diagonalization of the Hartree Hamiltonian for a given centre-of-mass configuration implies the following equation for the impurity dipole moment:

$$\boldsymbol{\mu}_i = \alpha_{i0}\boldsymbol{E}_i(1 + \alpha_{i0}^2|\boldsymbol{E}_i|^2/M_i^2)^{-1/2}. \tag{3.1}$$

In the absence of an external field, the local field at the impurity site is given by

$$\boldsymbol{E}_i = \sum_{j(\neq i)} \mathbf{T}_{ij} \cdot \boldsymbol{\mu}_j \tag{3.2}$$

where $\mathbf{T}_{ij} \equiv \mathbf{T}(\boldsymbol{R}_j - \boldsymbol{R}_i)$. We now diverge from the analysis of II, and assume dipolar polarizable solvent molecules, with total moment

$$\boldsymbol{\mu}_j = \boldsymbol{m}_0(j) + \boldsymbol{\alpha}_0(j) \cdot \boldsymbol{E}_j \qquad j \neq i \tag{3.3}$$

where the index j now refers to both the position and orientation of solvent molecule j; $\boldsymbol{m}_0(j)$ is the permanent dipole moment of the isolated solvent molecule, and the solvent polarizability is taken to be a tensor, $\boldsymbol{\alpha}_0(j)$, to allow for possible anisotropy. The local field at a solvent site, $\boldsymbol{E}_j$, is again given by (3.2).

To obtain an explicit expression for $\boldsymbol{E}_i$, for a given configuration of centre-of-mass positions and permanent moment orientations, we iterate (3.2) with the aid of (3.3), yielding

$$\boldsymbol{E}_i = \boldsymbol{\mathcal{G}} \cdot \boldsymbol{\mu}_i + \sum_j \boldsymbol{\mathcal{F}}(ij) \cdot \boldsymbol{m}_0(j). \tag{3.4}$$

The first term on the right-hand side is precisely that obtained in the case of a non-polar solvent, and describes the reaction field at the impurity due to $\boldsymbol{\mu}_i$. A microscopic prescription for $\boldsymbol{\mathcal{G}}$ is given in II. The second term describes the field due to the permanent dipoles of the solvent molecules, and the first few terms in $\boldsymbol{\mathcal{F}}(ij)$ are

$$\boldsymbol{\mathcal{F}}(ij) = \mathbf{T}_{ij} + \sum_k \mathbf{T}_{ik} \cdot \boldsymbol{\alpha}_0(k) \cdot \mathbf{T}_{kj} + \cdots . \tag{3.5}$$

More precisely, $\boldsymbol{\mathcal{F}}(ij)$ is the sum of all $\mathbf{T}$-tensor products that begin at the impurity site, end at the solvent site j, and do not have the impurity as an intermediate site. A product of n $\mathbf{T}$-tensors is associated with $n-1$ factors of $\boldsymbol{\alpha}_0(j)$.

It is clear from (3.1) that $\boldsymbol{E}_i$ and $\boldsymbol{\mu}_i$ are parallel, so that we can write

$$\boldsymbol{E}_i = \lambda \boldsymbol{\mu}_i \tag{3.6}$$

where λ is thus defined. For the special case of a non-polar solvent, it follows from (3.4) that $\boldsymbol{E}_i = \boldsymbol{\mathcal{G}} \cdot \boldsymbol{\mu}_i$, and we identify λ as one of the three eigenvalues of $\boldsymbol{\mathcal{G}}$ (see II). For the general case studied here, we use (3.6) to eliminate $\boldsymbol{E}_i$ from equations (3.1) and (3.4), yielding

$$\frac{|\boldsymbol{\mu}_i|^2}{M_i^2} = 1 - \frac{1}{\alpha_{i0}^2 \lambda^2} \tag{3.7}$$

$$\lambda \boldsymbol{\mu}_i = \boldsymbol{\mathcal{G}} \cdot \boldsymbol{\mu}_i + \sum_j \boldsymbol{\mathcal{F}}(ij) \cdot \boldsymbol{m}_0(j). \tag{3.8}$$

Equation (3.7) is formally identical to (2.18) of II.

Equation (3.8) constitutes an inhomogeneous matrix equation for $\boldsymbol{\mu}_i$, and in consequence $\boldsymbol{\mu}_i$ is invariably non-zero. Only in the limit of a non-polar solvent is the equation homogeneous, allowing a solution $\boldsymbol{\mu}_i = \mathbf{0}$. Thus, the local field at the impurity due to the permanent moments ensures a dipolar atomic impurity and, in contrast to the case of a non-polar solvent, there can be no strict transition from a non-polar impurity state to a dipolar Frenkel EI state. We expect, however, a changeover under appropriate conditions from a small impurity moment, arising from the random local field at the impurity, to a larger impurity moment, characteristic of the EI phase. We further expect this changeover to be rapid due to the co-operative effects that stabilize the impurity moment in the EI regime.

The solution of (3.7) and (3.8) yields values for $\boldsymbol{\mu}_i$ and λ for each configuration of site centre-of-mass positions and solvent moment orientations. Over the ensemble of such configurations, there are (correlated) distributions for the values of $\boldsymbol{\mu}_i$ and λ. In order to obtain a typical value of $|\boldsymbol{\mu}_i|$ with which to characterize the system for each set of input parameters, we suggest an extension of the mean field approximation of II. First, we calculate the ensemble average of the right-hand side of (3.8) with the magnitude and orientation of $\boldsymbol{\mu}_i$ held fixed at arbitrary values. For the special case of a non-polar solvent,

this is equivalent to replacing $\mathcal{G}$ by its ensemble average $\mathbf{G}$, which is precisely the mean field approximation of II. As we shall shortly show, the above average of the right-hand side of (3.8) is an odd function of μ_i, and we therefore write this quantity as $\langle\lambda\rangle_i\mu_i$, with $\langle\lambda\rangle_i$ a function of $|\mu_i|^2$. Equating this quantity with the left-hand side of (3.8), there are two possibilities. First, $\mu_i = \mathbf{0}$, corresponding to a non-dipolar impurity. Although the possibility of such a solution is a direct consequence of the mean field approximation, we interpret it as representing a situation in which there is only a small impurity moment arising from a random local field. The second solution is $\lambda = \langle\lambda\rangle_i$ which, when substituted into (3.7), yields the impurity dipole moment. Such a solution is interpreted as a true Frenkel EI phase, with the co-operative effects that stabilize the impurity dipole embodied in $\langle\lambda\rangle_i$. Thus, the mean field approximation replaces the continuous changeover in the nature of the impurity discussed above by a well defined transition.

To proceed with the mean field approximation, we consider a graphical analysis of the quantity $\langle\lambda\rangle_i$. As for the non-polar case studied in II, configurations of the system are weighted by a spherically symmetric reference potential. This was the only contribution to the Boltzmann factor considered in II, and here would lead to a zero contribution to $\langle\lambda\rangle_i$ from the second term on the right-hand side of (3.8). To obtain a non-zero contribution, we therefore include in addition the non-spherical dipolar interaction energy in the Boltzmann factor.

The Boltzmann factor for a given configuration can be written in terms of the many-particle Mayer f-function. Following the work of Wertheim on dipolar polarizable fluids [21–25], we expand the s-particle Mayer f-function for the full potential as

$$f_s(1\ldots s) = f_{R,s}(1\ldots s) + [1 + f_{R,s}(1\ldots s)]\sum_{n=1}^{\infty}[-\beta\phi_s(1\ldots s)]^n/n! \tag{3.9}$$

where $\beta = (kT)^{-1}$ is the inverse temperature, $f_{R,s}(1\ldots s)$ is the s-particle Mayer f-function for the reference potential, and $\phi_s(1\ldots s)$ is the s-particle dipolar interaction energy. The latter is the sum of all $\mathbf{T}$-bond chains connecting s points. If all points are solvent sites, then the $\mathbf{T}$-bond chain connects the permanent moments of two solvent sites. Alternatively, if the impurity site is one of the s points, then the $\mathbf{T}$-bond chain is such that the impurity does not form an interior stage, and the $\mathbf{T}$-bond chain either connects the permanent moments of two solvent molecules, or the impurity moment with the permanent moment of a solvent molecule. A product of n $\mathbf{T}$-tensors is associated with $n-1$ interior stages, each of which occurs with a factor of $\alpha_0(j)$.

The graphs contributing to $\langle\lambda\rangle_i$ thus include both a $\mathbf{T}$-bond chain from (3.8), and further chains from the $\phi_s(1\ldots s)$ terms of (3.9). In addition, there are $f_{R,s}(1\ldots s)$ connectors representing an average over the reference system. To analyse these complex graphs, it is convenient to make use of the following formal equivalence. In the model system, the isolated impurity is a polarizable atom with no intrinsic dipole moment, although one is stabilized in the EI phase. The above graphs are, however, reproduced precisely if we treat the impurity site as a non-polarizable atom with a constrained permanent moment, μ_i.

With this, we can make direct contact with Wertheim's work [21–25] on dipolar polarizable fluids, to which the reader is referred for much of the following notation. From his results it can be shown that:

$$\langle\lambda\rangle_i\mu_i = \beta^{-1}c(i). \tag{3.10}$$

The function c is precisely as defined by Wertheim, *with the proviso that the moment of site i takes the special value μ_i and the polarizability of site i is zero.* Consequently, the

impurity cannot be an interior stage of a **T**-bond chain. Specifically, $c(i)$ is the sum of all graphs free of 0-AP with one extra chain which leaves the graph at i, any number of chains connecting permanent moments, and h_2 bonds (which represent the average over the reference system).

For the special case of a non-polar solvent, the only moment is that on the impurity site, μ_i; $c(i)$ then consists of graphs with one extra chain, which begins at site i and leaves the graph at i, and any number of chains that begin and end at site i. It is these latter chains, which describe the contribution of the dipolar interaction energy to the Boltzmann factor, that were neglected in the analysis of II. As we shall shortly see, these chains do not contribute in a linear theory.

Returning to the case of a polar solvent, the presence of an extra chain means that the total number of factors of the permanent moments contributing to each graph in $c(i)$ must be odd. Since every solvent site must occur with an even number of permanent moments (otherwise the integration over the orientation of that point would yield zero), $c(i)$ must be an odd function of μ_i, and consequently $\langle\lambda\rangle_i$ is an even function of μ_i. In practice, we later neglect graphs in $c(i)$ that are non-linear in μ_i, whence $\langle\lambda\rangle_i$ is independent of μ_i, and we recover solutions of the form (2.2). More generally, $\langle\lambda\rangle_i$, and hence the self-consistency relation for μ_i, constitutes an infinite-order polynomial in μ_i.

In order to find an expression for $\langle\lambda\rangle_i$, it is convenient to perform a topological reduction of the graphs contributing to $c(i)$, using the two levels of renormalization described by Wertheim [23]. The 1-R renormalization results in graphs free of 1-AP, and with factors of $m_0(j)$ replaced by

$$m(j) = m_0(j) + \beta^{-1}\alpha_0(j) \cdot c(j). \tag{3.11}$$

The renormalized dipole moment, $m(j)$, is enhanced relative to that of the isolated molecule, $m_0(j)$, due to interactions with surrounding molecules embodied in the second term of (3.11). In 1-R form, $c(i)$ is identical to the function $w(i)$ introduced by Wertheim [23]. The 2-R renormalization results in graphs free of 2-AP, and with factors of $\alpha_0(j)$ replaced by the renormalized polarizability

$$\alpha(j) = \alpha_0(j) + \beta^{-1}\alpha_0(j) \cdot \mathbf{C}(j) \cdot \alpha_0(j) \tag{3.12}$$

where

$$\mathbf{C}(j) = \frac{\partial c(j)}{\partial m_0(j)}. \tag{3.13}$$

In 2-R form, $c(i)$ is identical to the function $y(i)$ of Wertheim [23]. In fact, the 2-R renormalization requires an additional correction to properly account for ring-chains [23], but since this is not required for the linear theories we consider below, we do not go into it here. In general, the above renormalizations apply to all stages of a graph, but because we have taken the impurity to be formally non-polarizable, the renormalizations (3.11) and (3.12) apply only to the solvent sites.

In 2-R form, $\langle\lambda\rangle_i\mu_i = \beta^{-1}y(i)$ can thus be written in terms of graphs free of 0-AP, 1-AP and 2-AP, with a renormalized solvent permanent moment, $m(j)$, and a renormalized solvent polarizability, $\alpha(j)$. We now make the restriction to linear theories, which we define to be as follows. Each graph contributing to $y(i)$ consists of h_2-connectors associated with the reference potential, and a single superchain that begins at i and leaves the graph at i. A superchain is defined [21] as a chain of chains placed end-to-end, and we assume here the constituent chains to be linear, in the sense that each solvent site is associated with only

one stage of the chain. With the assumption of a linear theory, the distinction between the $y(i)$ function defined here and that of Wertheim disappears, since neither includes graphs with interior stages at i.

Every graph is thus assumed to be linear in μ_i, i.e. we ignore graphs in μ_i^{2n+1}, $n = 1, 2 \ldots$. Further, every solvent site is assumed to be associated with at most either a factor of $m(j)m(j)$, if two chains meet at the site, or a factor of $\alpha(j)$, if the site is an interior stage of a chain. With the assumed linearity of $y(i)$ in μ_i, we define a μ_i-independent tensor $\mathbf{Y}(i)$ via $y(i) = \mathbf{Y}(i) \cdot \mu_i$. The quantity of interest, $\langle\lambda\rangle_i$, is thus obtained from

$$\langle\lambda\rangle_i \mu_i = \beta^{-1}\mathbf{Y}(i) \cdot \mu_i \tag{3.14}$$

and can be identified as an eigenvalue of $\beta^{-1}\mathbf{Y}(i)$.

Considering the non-polar case, with $m(j) = \mathbf{0}\ \forall j$, the only non-zero superchain is that consisting of a single extra chain, and the function $\beta^{-1}\mathbf{Y}(i)$ is found to be formally identical to the average reaction field factor, $\mathbf{G}$, studied in II. Averaging over the solvent orientations, and consequently replacing $\alpha(j)$ by α, we thus recover the linear theories evaluated in section 2.

In the case of a polar solvent, for each graph in which solvent site j is associated with a factor of $\alpha(j)$, there is another graph identical to the first except that solvent site j is associated with a factor of $m(j)m(j)$. For the polar case, we therefore obtain all graphs in $\beta^{-1}\mathbf{Y}(i)$ from those corresponding to the non-polar case by replacing each factor of $\alpha(j)$ at the solvent sites by $\alpha(j) + \beta m(j)m(j)$, (the factor of β arises from the additional chain implied). With only one stage at each solvent site, the average over solvent orientations is trivial. The orientational average of $m(j)m(j)$ yields $(1/3)m^2\mathbf{I}$, and that of $\alpha(j)$ yields $\alpha\mathbf{I}$, where $m = |m|$ and $\alpha = (1/3)\mathrm{Tr}[\alpha]$. The function $\beta^{-1}\mathbf{Y}(i)$ is thus identical to $\mathbf{G}$, with the replacement of α by $\alpha + (1/3)\beta m^2$.

The (triply degenerate) eigenvalue of $\beta^{-1}\mathbf{Y}(i)$ is thus

$$\langle\lambda\rangle_i = G[\alpha + (1/3)\beta m^2]. \tag{3.15}$$

Equation (3.15) is the central result of the preceding graphical analysis. For $\alpha_{i0}G[\alpha + (1/3)\beta m^2] > 1$, we simply replace λ in (3.7) by $\langle\lambda\rangle_i$, as given by (3.15). We thus recover (2.2) for the impurity moment in the Frenkel EI phase, with $G(\alpha)$ replaced by $G[\alpha + (1/3)\beta m^2]$. When $\alpha_{i0}G[\alpha + (1/3)\beta m^2] < 1$, however, the only solution is the trivial solution, $\mu_i = \mathbf{0}$, corresponding to the non-dipolar state of (2.1). The mean field approach thus gives a transition from a normal insulating phase to an EI phase when $\alpha_{i0}G[\alpha + (1/3)\beta m^2] = 1$. As argued above, this well defined transition is assumed to reflect the sharp but continuous increase in μ_i which a more rigorous analysis would reveal.

Given a specific linear theory, we obtain G as a function of $\alpha + (1/3)\beta m^2$, and knowledge of G is sufficient to follow the evolution of the impurity dipole moment, via (2.1) and (2.2). The final task, therefore, is to obtain expressions for m and α. For linear theories, (3.13) implies that $c(j) = \mathbf{C}(j) \cdot m_0(j)$, and we thus rewrite (3.11) as

$$m(j) = m_0(j) + \beta^{-1}\alpha_0(j) \cdot \mathbf{C}(j) \cdot m_0(j). \tag{3.16}$$

For a solvent site, it can be shown that

$$\beta^{-1}\alpha_0(j) \cdot \mathbf{C}(j) = G\alpha(j) \tag{3.17}$$

and consequently, (3.16) and (3.12) reduce to

$$m(j) = m_0(j) + G\alpha(j) \cdot m_0(j) \tag{3.18}$$

$$\alpha(j) = \alpha_0(j) + G\alpha(j) \cdot \alpha_0(j). \tag{3.19}$$

Equations (3.18) and (3.19) yield $m(j)$ and $\alpha(j)$ in terms of $G \equiv G[\alpha+(1/3)\beta m^2]$, which is sufficient to close the problem.

The expression $\alpha + (1/3)\beta m^2$ takes on a simple form when we consider a special, but common, situation. We suppose that the principal axes of $\alpha_0(j)$ are mutually orthogonal, with one lying parallel to the permanent moment $m_0(j)$; $\alpha_0(j)$ is hence diagonal, with component $\alpha_{0\|}$ parallel to the moment and components $\alpha_{0\perp}$ perpendicular to the moment. Equations (3.18) and (3.19) then reduce to

$$\alpha + (1/3)\beta m^2 = \frac{1}{3}\left(\frac{\alpha_{0\|}}{1-G\alpha_{0\|}} + \frac{2\alpha_{0\perp}}{1-G\alpha_{0\perp}} + \frac{\beta m_0^2}{(1-G\alpha_{0\|})^2}\right). \tag{3.20}$$

3.2. Results

We now give results appropriate to a solvent of polar polarizable molecules. As discussed above, for the linear theories that we consider, the sole difference resulting from the inclusion of permanent dipole moments on the solvent sites is the replacement of α by $\alpha+(1/3)\beta m^2$ in the corresponding calculation for a non-polar solvent. There is hence no qualitative difference between the polar and non-polar cases, and the trends described in section 2 are again observed. There is, however, a significant quantitative difference, arising from the fact that $(1/3)\beta m_0^2$ is appreciably larger than α_0 for many polar solvents. For example, at 263 K, $(1/3)\beta m_0^2 = 19.8\,\text{Å}^3$ and $\alpha_0 = 2.2\,\text{Å}^3$ for ammonia; and $(1/3)\beta m_0^2 = 15.8\,\text{Å}^3$ and $\alpha_0 = 4.7\,\text{Å}^3$ for methylamine [26]. For the present model, therefore, the probability of a Frenkel EI phase is greatly enhanced for a polar polarizable solvent.

As in section 2.2, we assume the reference interaction potential to be of hard-sphere form, with a hard-sphere diameter that is different for impurity–solvent and solvent–solvent interactions. For this reason, we again consider the MSA. The impurity dipole moment is thus given by (2.1) or (2.2), and (2.21), with $\tilde{\alpha}$ replaced by $\tilde{\alpha}+(1/3)m^{*2}$, where $m^{*2} = \beta m^2/\sigma_{ss}^3$. This replacement must also be employed in the calculation of G^{ss}. With the assumptions described before, we take $\tilde{\alpha} + (1/3)m^{*2}$ to be given from (3.20).

Since the qualitative trends are precisely as described in section 2, we present here only a limited series of example calculations. We take parameters appropriate to the alkali metals in methylamine at a single temperature and density. We stress that this is an illustrative calculation only, designed to show that a Frenkel EI phase is a valid possibility. In no way do we intend to provide the final solution to the complex chemistry of these systems!

Methylamine possesses a dipole moment of 1.31 D [26], and a scalar polarizability of $4.7\,\text{Å}^3$ [26] (we neglect the anisotropy of the polarizability). We assume a temperature of 263 K, for which the density of methylamine is $0.699\,\text{g cm}^{-3}$ [27]. We must estimate a value for the hard-sphere diameter of methylamine, the quantity most prone to uncertainty. From the known bond lengths and angles [26], we adopt the rough estimate, $\sigma_{ss} = 4.2$ Å. With these parameters, we find $\rho^* = 1.002$, $m_0^* = 0.799$ and $\tilde{\alpha}_0 = 0.063$.

From the solution of the MSA [21], we predict a dielectric constant of 10.4 at $T = 263$ K for the pure solvent, which is reasonably close to the experimental value of 11.4 [26]. The ability of the MSA to reproduce the observed dielectric constant for a variety of liquids has been noted before (see, for example, [28]), and undoubtedly arises from a fortuitous cancellation. The MSA is known to underestimate the dielectric constant of a dipolar model liquid, but real liquids often have appreciable quadrupole moments which depress the dielectric constant to a value comparable with the MSA prediction. Our modelling of methylamine should not therefore be taken too seriously although, for whatever reason, it

does seem to reproduce the dielectric properties adequately. We note that the renormalized dipole moment and polarizability of the solvent molecule are $m^* = 0.886$ and $\tilde{\alpha} = 0.070$, showing a small increase on the unrenormalized values.

The alkali metal atoms have polarizabilities of 24 $Å^3$ (Li), 24 $Å^3$ (Na), 43 $Å^3$ (K), 48 $Å^3$ (Rb) and 60 $Å^3$ (Cs) [20], and thus $\tilde{\alpha}_{i0} = 0.324$ (Li), 0.324 (Na), 0.580 (K), 0.648 (Rb) and 0.810 (Cs). It is known [29, 30] that the static structure factor of the alkali metals at their melting points can be fitted closely by the Percus–Yevick result for hard spheres at a packing fraction of 0.45. From the densities of the alkali metals at their melting points, we may therefore estimate the following effective hard-sphere diameters: $\sigma_{ii} = 2.68$ Å (Li), 3.27 Å (Na), 4.08 Å (K), 4.40 Å (Rb) and 4.67 Å (Cs). The corresponding values of Σ are 0.638 (Li), 0.779 (Na), 0.971 (K), 1.048 (Rb) and 1.112 (Cs).

With the above parameters for the alkali impurities, we find a dipole moment $\mu_i/M_i = 0.296$ for Li, and $\mu_i/M_i = 0.285$ for Cs; Na, K and Rb are predicted to be non-dipolar. With $M_i \approx 6D$ (Li) and $M_i \approx 8D$ (Cs) [31], the predicted dipole moments for Li and Cs are $1.8D$ and $2.3D$ respectively. These dipole moments are significantly larger than that of the methylamine molecule. As discussed in section 2, a dipolar impurity state is favoured by a large impurity polarizability and a small impurity diameter. Clearly, Cs is dipolar for the former reason, and Li for the latter. The remaining alkali species, although predicted to be non-polar, are in fact close to the EI instability.

4. Summary

In this paper we have presented numerical results for the atomic dipole moment, characterizing the dipolar Frenkel EI phase, of an impurity in a liquid solvent. Because of the approximations employed, these calculations are expected to give merely a rough estimate of the situations in which a Frenkel EI phase may occur. As discussed in detail in II, however, the mean field approximation we have used is likely, if anything, to underestimate the occurrence of an EI phase. For a non-polar solvent, we found (sections 2.1 and 2.2) an EI phase for a few of the more favourable choices of parameters characterizing the solvent and impurity species. An EI phase was found, however, to be much more likely for a polar solvent (see section 3), where the permanent moments of the solvent molecules significantly enhance the reaction field at the impurity.

The experimental quantities that distinguish a Frenkel EI phase, and some competing effects that are not included in the model system, have been discussed in II. It is clear from the results of this paper that an EI phase is favoured by a solvent that is dense, highly polar and highly polarizable, i.e. a high dielectric constant solvent. It is known [10], however, that for solvents with a very high dielectric constant, the impurity often ionizes completely, an effect not included in the model. The best solvents are therefore likely to be those with an intermediate value of the dielectric constant. As an example, we selected parameters appropriate to the alkali metals in methylamine, and found that, at the temperature considered, a dipolar state would exist for Li and Cs.

Acknowledgments

This work was supported by British Petroleum VRU. MDW is also grateful for the award of a Research Fellowship from the Royal Commission for the Exhibition of 1851. Useful discussions with Professor P P Edwards and Dr G Kahl are gratefully acknowledged.

Appendix. MSA solution for unequal impurity and solvent diameters

The solution of the MSA for an isolated impurity atom in a solvent of different diameter can be obtained from the solution of the corresponding binary mixture in the limit that the concentration of the impurity species tends to zero. The MSA for a binary mixture of non-polarizable dipolar molecules, to which the current problem is formally equivalent, has been solved by Adelman and Deutch [32] for the case of equal hard-sphere diameters, and by Isbister and Bearman [33] for the case of unequal diameters (see also [34]). The solution of Isbister and Bearman, in the appropriate limit, was used by Nichols and Calef [35] to study the solvation dynamics of a dipole in a dipolar solvent within the MSA. With appropriate modifications, the results of Nichols and Calef can be used here. Since the context is rather different, we give here a derivation of the result used in section 2.2.

We denote the average reaction field factor appropriate to the isolated impurity in the solvent by $\mathbf{G}^{is} = G^{is}\mathbf{I}$. For any linear theory, a graphical analysis of $\mathbf{G}^{is}$ leads to the following set of relations:

$$\mathbf{G}^{is} = \rho\alpha \int \mathrm{d}(\boldsymbol{R})\, \mathbf{T}(\boldsymbol{R})\mathbf{H}^{is}(-\boldsymbol{R}) \tag{A.1}$$

$$\mathbf{H}^{is} = \mathbf{C}^{is} + \rho\alpha\mathbf{C}^{is} * \mathbf{H}^{ss} \tag{A.2}$$

$$\mathbf{H}^{ss} = \mathbf{C}^{ss} + \rho\alpha\mathbf{C}^{ss} * \mathbf{H}^{ss}. \tag{A.3}$$

Here, ρ is the solvent density, α is the renormalized solvent polarizability, $\mathbf{T}(\boldsymbol{R})$ is defined in (2.5), ' $*$ ' denotes a spatial convolution, and $\mathbf{H}$ and $\mathbf{C}$ are the functions introduced by Wertheim [12]. The superscript 'is' refers to a function connecting the impurity to a solvent molecule, and the superscript 'ss' refers to a function connecting two solvent molecules. The impurity–solvent and solvent–solvent $\mathbf{H}$ and $\mathbf{C}$ functions differ only in the required reference potential, and are identical in the limit of equisized hard spheres. Note that all contributions to $\mathbf{G}^{is}$ are short-ranged, and the integrations may be extended over all space.

Because of the symmetry of the dipole–dipole interaction, we look for solutions of the form

$$\mathbf{H}^{is}(\boldsymbol{R}) = H_I^{is}(R)\mathbf{I} + H_T^{is}(R)\mathbf{T}_0(\boldsymbol{R}) \tag{A.4}$$

where $\mathbf{T}_0(\boldsymbol{R}) = R^3\mathbf{T}(\boldsymbol{R})$, and with analogous expressions for $\mathbf{H}^{ss}(\boldsymbol{R})$, $\mathbf{C}^{is}(\boldsymbol{R})$ and $\mathbf{C}^{ss}(\boldsymbol{R})$. Inserting (A.4) into (A.1), we find

$$G^{is} = 8\pi\rho\alpha \int_0^\infty \mathrm{d}R\, R^{-1} H_T^{is}(R) = 8\pi\rho\alpha K^{is} \tag{A.5}$$

where K^{is} is thus defined.

Assuming the form of (A.4), equations (A.2) and (A.3) reduce in the standard way [12] to

$$H_+^{is} = C_+^{is} + 6\rho\alpha K^{ss} C_+^{is} * H_+^{ss} \tag{A.6}$$

$$H_-^{is} = C_-^{is} - 3\rho\alpha K^{ss} C_-^{is} * H_-^{ss} \tag{A.7}$$

$$H_+^{ss} = C_+^{ss} + 6\rho\alpha K^{ss} C_+^{ss} * H_+^{ss} \tag{A.8}$$

$$H_-^{ss} = C_-^{ss} - 3\rho\alpha K^{ss} C_-^{ss} * H_-^{ss} \tag{A.9}$$

where H_+^{is}, etc. are defined via

$$H_I^{is} = K^{is}(2H_+^{is} - 2H_-^{is}) \tag{A.10}$$

$$\hat{H}_T^{is} = K^{is}(2H_+^{is} + H_-^{is}) \tag{A.11}$$

$$H_I^{ss} = K^{ss}(2H_+^{ss} - 2H_-^{ss}) \tag{A.12}$$

$$\hat{H}_T^{ss} = K^{ss}(2H_+^{ss} + H_-^{ss}) \tag{A.13}$$

and similarly for the C functions. The function $\hat{H}_T^{is}(R)$ is given by

$$\hat{H}_T^{is}(R) = H_T^{is}(R) - 3\int_R^\infty dR'\, R'^{-1} H_T^{is}(R') \tag{A.14}$$

with analogous expressions for $\hat{H}_T^{ss}$, $\hat{C}_T^{is}$ and $\hat{C}_T^{ss}$. The transformation (A.14) has the inverse

$$H_T^{is}(R) = \hat{H}_T^{is}(R) - \frac{3}{R^3}\int_0^R dR'\, R'^2 \hat{H}_T^{is}(R'). \tag{A.15}$$

The term K^{ss} is defined in terms of $H_T^{ss}(R)$ in an analogous way to (A.5), and a function G^{ss} may correspondingly be defined.

The above analysis applies to any linear theory. To obtain explicit solutions, however, we need to supplement the Ornstein–Zernike analogues (A.2) and (A.3) with approximate closure relations, and we take those appropriate to the MSA (i.e. Wertheim's SSCA [12] with the hard sphere $g_2(R)$ taken to be a step function):

$$\mathbf{H}^{is}(R) = \mathbf{0} \qquad R < \sigma_{is} \tag{A.16}$$

$$\mathbf{H}^{ss}(R) = \mathbf{0} \qquad R < \sigma_{ss} \tag{A.17}$$

$$\mathbf{C}^{is}(R) = \mathbf{T}(R) \qquad R > \sigma_{is} \tag{A.18}$$

$$\mathbf{C}^{ss}(R) = \mathbf{T}(R) \qquad R > \sigma_{ss}. \tag{A.19}$$

Here, σ_{is} and σ_{ss} are the hard-sphere diameters defined in section 2.2. Using (A.4) and the subsequent transformations, these closure relations reduce to

$$H_+^{is}(R) = H_-^{is}(R) = -1 \qquad R < \sigma_{is} \tag{A.20}$$

$$H_+^{ss}(R) = H_-^{ss}(R) = -1 \qquad R < \sigma_{ss} \tag{A.21}$$

$$C_+^{is}(R) = C_-^{is}(R) = 0 \qquad R > \sigma_{is} \tag{A.22}$$

$$C_+^{ss}(R) = C_-^{ss}(R) = 0 \qquad R > \sigma_{ss}. \tag{A.23}$$

Equations (A.6) and (A.8) for the + functions, together with the above closure relations, correspond to the Percus–Yevick equations for a binary hard-sphere mixture, for which one component (the solvent) is at an effective density of $6\rho\alpha K^{ss}$ and the other component (the impurity) is at an infinitesimal density. The same situation holds for the − functions, except that the effective solvent density is now $-3\rho\alpha K^{ss}$. The Percus–Yevick equations for a binary hard-sphere mixture were first solved by Lebowitz [36], who gave analytical expressions for the direct correlation functions (in the present context, $C_+^{is}(R)$ etc.) for R less than the hard-sphere radius. We now make use of these expressions.

It is clear from (A.5) that the aim is to calculate K^{is}, and a convenient route to this quantity is the following. Consider the appropriate expression (A.15) for $C_T^{is}(R)$, and

for $R > \sigma_{is}$. Using the closure relations and the appropriate transformation (A.11), this expression reduces to

$$1 = -6K^{is}\int_0^{\sigma_{is}} dR\, R^2 C_+^{is}(R) - 3K^{is}\int_0^{\sigma_{is}} dR\, R^2 C_-^{is}(R). \tag{A.24}$$

As stated above, $C_+^{is}(R)$ and $C_-^{is}(R)$ are the appropriate solutions of the Percus–Yevick equations for the mixture, with an effective solvent density of $6\rho\alpha K^{ss}$ and $-3\rho\alpha K^{ss}$ respectively. We may thus write (A.24) as

$$\frac{K^{ss}}{K^{is}} 4\pi\rho\alpha = q^{is}(\pi\rho\alpha K^{ss}\sigma_{ss}^3) - q^{is}(-\pi\rho\alpha K^{ss}\sigma_{ss}^3/2) \tag{A.25}$$

where

$$q^{is}(\eta) = 1 - 24\eta\sigma_{ss}^{-3}\int_0^{\sigma_{is}} dR\, R^2 C_{PY}^{is}(R) \tag{A.26}$$

and $C_{PY}^{is}(R)$ is the impurity–solvent Percus–Yevick direct correlation function for solvent packing fraction $\eta = \pi\rho\sigma_{ss}^3/6$. Relating K^{is} to G^{is} via (A.5), and K^{ss} to G^{ss} similarly, we rearrange (A.25) to

$$G^{is} = \frac{4\pi\rho\alpha G^{ss}}{q^{is}(G^{ss}\sigma_{ss}^3/8) - q^{is}(-G^{ss}\sigma_{ss}^3/16)}. \tag{A.27}$$

As stated previously, with equisized hard spheres the H and C functions are the same for both impurity–solvent and solvent–solvent cases. Hence, G^{ss} may be interpreted as the average reaction field factor for the impurity obtained in the equisized hard-sphere case; α is purely a property of the solvent, and is the same as for the equisized case.

All that remains, therefore, is to find an expression for $q^{is}(\eta)$. Integrating over the Percus–Yevick expression [36] for the impurity–solvent direct correlation function in the limit of zero impurity density, one finds the following expression for $q^{is}(\eta)$ in terms of the ratio $\Sigma = \sigma_{il}/\sigma_{ss}$:

$$q^{is}(\eta) = 1 + 24\eta\left(a_s(\eta)\frac{(\Sigma+1)^3}{24} + b(\eta)\frac{(\Sigma+1)(2\Sigma+1)}{24} + d(\eta)\frac{(3\Sigma^2-1)}{12}\right) \tag{A.28}$$

where the coefficients are given by

$$a_s(\eta) = \frac{(1+2\eta)^2}{(1-\eta)^4} \tag{A.29}$$

$$b(\eta) = \frac{-3\eta(2+\eta)[1+\eta(2\Sigma-1)/(\Sigma+1)]}{(1-\eta)^4} \tag{A.30}$$

$$d(\eta) = \frac{\eta(1+2\eta)^2}{2(1-\eta)^4}. \tag{A.31}$$

Note that, although the Lebowitz solution [36] yields different expressions for $C_{PY}^{is}(R)$ for the cases $\Sigma < 1$ and $\Sigma > 1$, the resulting expressions for $q^{is}(\eta)$ are identical. The final equations for G^{is}, (A.27)–(A.31), can be shown to be equivalent to (6) of [35].

References

[1] Winn M D and Logan D E 1992 *J. Phys.: Condens. Matter* **4** 5509
[2] Winn M D and Logan D E 1993 *J. Phys.: Condens. Matter* submitted
[3] Logan D E 1987 *J. Chem. Phys.* **86** 234
[4] Chenier J H B, Howard J A, Joly H A and Mile B 1990 *J. Chem. Soc. Faraday Transactions* **86** 2169
[5] Schindelbeck Th, Nattland D and Freyland W 1991 *J. Physique IV* **1** C5-155
[6] Xu L F, Selloni A and Parrinello M 1989 *Chem. Phys. Lett.* **162** 27
[7] Sprik M, Impey R W and Klein M L 1986 *Phys. Rev. Lett.* **56** 2326
[8] Martyna G J and Klein M L 1992 *J. Chem. Phys.* **96** 7662
[9] Logan D E 1986 *Phys. Rev. Lett.* **57** 782
[10] Edwards P P 1982 *Adv. Inorg. Chem. Rad.* **25** 135
[11] Onsager L 1939 *J. Phys. Chem.* **43** 189
[12] Wertheim M S 1973 *Mol. Phys.* **25** 211
[13] Patey G N 1977 *Mol. Phys.* **34** 427
[14] Pratt L R 1980 *Mol. Phys.* **40** 347
[15] Rushbrooke G S, Stell G and Høye J S 1973 *Mol. Phys.* **26** 1199
[16] Verlet L and Weiss J J 1972 *Phys. Rev.* A **5** 939
[17] Barker J A, Henderson D and Smith W R 1968 *Phys. Rev. Lett.* **21** 134
[18] Chandler D, Schweizer K S and Wolynes P G 1982 *Phys. Rev. Lett.* **49** 1100
[19] Bottcher C J F 1973 *Theory of Electric Polarization* (Amsterdam: Elsevier) 2nd edn
[20] Radzig A A and Smirnov B M 1985 *Reference Data on Atoms, Molecules and Ions* (Berlin: Springer)
[21] Wertheim M S 1973 *Mol. Phys.* **26** 1425
[22] Wertheim M S 1977 *Mol. Phys.* **33** 95
[23] Wertheim M S 1977 *Mol. Phys.* **34** 1109
[24] Wertheim M S 1978 *Mol. Phys.* **36** 1217
[25] Wertheim M S 1979 *Mol. Phys.* **37** 83
[26] 1992 *CRC Handbook of Chemistry and Physics* (New York: CRC) 73rd edn
[27] 1982 *Dictionary of Organic Compounds* (London: Chapman and Hall) 5th edn
[28] Stell G, Patey G N and Høye J S 1981 *Adv. Chem. Phys.* **48** 183
[29] Ashcroft N W and Lekner J 1966 *Phys. Rev.* **145** 83
[30] Hansen J-P and McDonald I R 1986 *Theory of Simple Liquids* (New York: Academic) 2nd edn
[31] Teachout R R and Pack R T 1971 *Atomic Data* **3** 195
[32] Adelman S A and Deutch J M 1973 *J. Chem. Phys.* **59** 3971
[33] Isbister D and Bearman R J 1974 *Mol. Phys.* **28** 1297
[34] Cummings P T and Blum L 1986 *J. Chem. Phys.* **85** 6658
[35] Nichols A L and Calef D F 1988 *J. Chem. Phys.* **89** 3783
[36] Lebowitz J L 1964 *Phys. Rev.* A **133** 895